A single topical dose of erythropoietin applied on a collagen carrier enhances calvarial bone healing in pigs

Jan Hendrik Duedal Rölfing[1,2], Jonas Jensen[1], Julie Neerup Jensen[1], Anne-Sofie Greve[1], Helle Lysdahl[1], Muwan Chen[1], Lars Rejnmark[3], and Cody Bünger[1,2]

[1]Orthopaedic Research Laboratory; [2]Department of Orthopaedics; [3]Department of Endocrinology and Internal Medicine, Aarhus University Hospital, Aarhus, Denmark.
Correspondence: jan.roelfing@ki.au.dk
Submitted 13-08-21. Accepted 13-12-02

Background and purpose — The osteogenic potency of erythropoietin (EPO) has been documented. However, its efficacy in a large-animal model has not yet been investigated; nor has a clinically safe dosage. The purpose of this study was to overcome such limitations of previous studies and thereby pave the way for possible clinical application. Our hypothesis was that EPO increases calvarial bone healing compared to a saline control in the same subject.

Methods — We used a porcine calvarial defect model. In each of 18 pigs, 6 cylindrical defects (diameter: 1 cm; height: 1 cm) were drilled, allowing 3 pairwise comparisons. Treatment consisted of either 900 IU/mL EPO or an equal volume of saline in combination with either autograft, a collagen carrier, or a polycaprolactone (PCL) scaffold. After an observation time of 5 weeks, the primary outcome (bone volume fraction (BV/TV)) was assessed with high-resolution quantitative computed tomography. Secondary outcome measures were histomorphometry and blood samples.

Results — The median BV/TV ratio of the EPO-treated collagen group was 1.06 (CI: 1.02–1.11) relative to the saline-treated collagen group. Histomorphometry showed a similar median effect size, but it did not reach statistical significance. Autograft treatment had excellent healing potential and was able to completely regenerate the bone defect independently of EPO treatment. Bony ingrowth into the PCL scaffold was sparse, both with and without EPO. Neither a substantial systemic effect nor adverse events were observed. The number of blood vessels was similar in EPO-treated defects and saline-treated defects.

Interpretation — Topical administration of EPO on a collagen carrier moderately increased bone healing. The dosing regime was safe, and could have possible application in the clinical setting. However, in order to increase the clinical relevance, a more potent but still clinically safe dose should be investigated.

Erythropoietin (EPO) is a hematopoietic growth factor that stimulates the formation of red blood cells. In recent years, the non-hematopoietic effects of EPO have been investigated. Of interest for skeletal tissue engineering, the pleiotropic capabilities of EPO include osteogenic and angiogenic potencies (Rölfing et al. 2012). Subcutaneous injections of 250 IU/kg EPO were found to enhance bone formation 6 weeks after operation in a spinal fusion model in rabbits (Rölfing et al. 2012). The validity of the methodology of this study was confirmed in a recently published meta-analysis (Riordan et al. 2013, Rölfing and Bünger 2013). Other independent research groups have reported increased bone formation in mice and rats after daily treatment with 200–6,000 IU/kg EPO (Bozlar et al. 2006, Holstein et al. 2007, 2011, Shiozawa et al. 2010, Garcia et al. 2011, Kim et al. 2012). Furthermore, vascularization of 3-dimensional scaffolds for bone tissue regeneration remains a challenge. The described pleiotropic functions of EPO may overcome this limitation of skeletal tissue engineering in the future. EPO could possibly facilitate angiogenesis directed into the core of the scaffold, thereby facilitating bony ingrowth. Moreover, EPO promotes a direct and indirect osteogenic stimulation of mesenchymal stromal cells (Shiozawa et al. 2010, Rölfing et al. 2013).

Translation of these promising in vitro and in vivo data into clinical trials requires a physiological dosage of EPO in order to avoid its known complications, such as thromboembolism (Ehrenreich et al. 2009, Shiozawa et al. 2010, Kim et al. 2012, Rölfing et al. 2012). Notably, we observed an extremely high hematocrit level after 250 IU/kg EPO for 20 days in a rabbit model (Rölfing et al. 2012). In other in vivo studies, repetitive EPO injections ranging from 500 to 6,000 IU/kg were administered. These treatment regimes have a systemic effect, and thus hold the risk of adverse events. Testing of the efficacy

DOI 10.3109/17453674.2014.889981

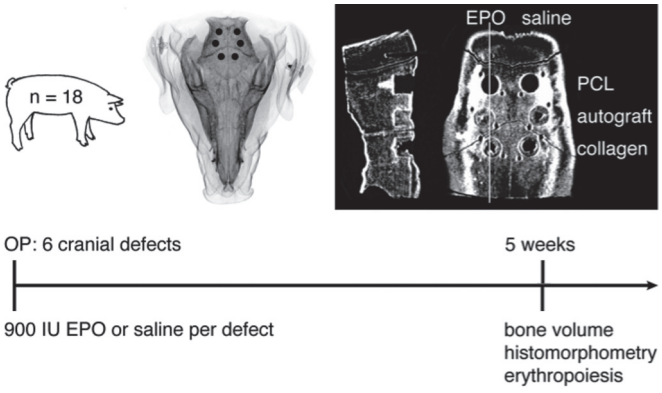

Figure 1. The study design and the positioning of the bone defects.

of a clinically safe dose of EPO is therefore necessary before clinical trials can be considered. Aiming for clinical progress and feasibility, the present study was carried out with a view to evaluating the efficacy of a single, low-dose EPO to stimulate bone healing in a large-animal study. The dose of EPO was chosen based on the following considerations. The translation of the minimally effective dose in cell studies into large-animal models is difficult (Rölfing et al. 2013). The rather low dosage of 2,700 IU/animal, equivalent to 18.5 ± 2.0 IU/kg, was chosen in order to minimize the systemic effect of EPO due to safety concerns and in order to minimize the potential effect on the within-subject controls. In anemic patients, 20–240 IU/kg are injected subcutaneously or intravenously 3 times a week. The hypothesis was that 900 IU site-specifically applied EPO would increase bony ingrowth compared to a saline-treated control in a porcine calvarial defect model.

Materials and methods

Study design

We used 18 female adolescent pigs (mean age 193 (SD 11) days, mean weight 146 (SD 16) kg) of breed (Danish Landrace × Yorkshire) × Duroc in this paired, block-randomized study to compare 6 groups in a cranial bone defect model. The within-subject study design eliminated the variability caused by biological variation among animals.

The treatment groups consisted of autograft ± EPO, collagen scaffold ± EPO, and PCL scaffold ± EPO (Figure 1). No empty defect was investigated because 3 pairwise comparisons investigating the effect of EPO compared to saline were planned. A carrier that absorbed and contained the liquid within the defect was therefore required. A collagen carrier was chosen, guided by previous studies (Stockmann et al. 2012, Schmitt et al. 2013).

Systematic influence from potential, undetected site-dependent differences was avoided by alternating the placement of the groups between animals. Choosing a sample size of 18 pigs allowed each treatment group to be represented at each bone defect site 3 times. Randomization was performed by generating random numbers. First, EPO was randomized to either the left or the right side of the calvaria (1 = right side and 2 = left side), and then the 3 pairs were randomized to either 1 = anterior, 2 = middle, or 3 = posterior location. However, the placement allocation was limited to 3 times per defect site. These measures ensured that any of the 6 possible combinations were present at each location 3 times, thereby potential site-dependent differences or any local influence of neighboring implants would add to the data variance rather than bias the results (Baas 2008). All experiments complied with local laws and were approved by the Danish National Authority (no. 2012-15-2934-00362).

Erythropoietin (EPO)

Epoetin beta (EU/1/97/031/032, NeoRecormon batch H6201H06; Roche, Welwyn Garden City, UK) was diluted with isotonic saline (9 mg/mL NaCl) to a concentration of 3,000 IU/mL immediately before administration (Bleuel et al. 1996). The timing of EPO dilution is important because the company states that the concentration of polysorbate 20 contained in the drug solution is critical for the stability of EPO; if the concentration of this detergent is too low, EPO will quickly adsorb to the surfaces of the drug container and will not be available for administration. Each defect received 900 IU EPO or an equal volume of saline.

To avoid biological interaction between the treatment and control groups, the 3 EPO groups and 3 control groups were kept apart on either the right or the left side according to randomization. Furthermore, the distance between the bone defects was at least 1 cm and the autograft and PCL scaffold groups were sealed with bone wax. Approximately 5 mm × 5 mm bone wax (Aesculap AG, Tuttlingen, Germany) was cut and molded into a flat, thin seal that was then pressed onto the surface of the autograft and PCL scaffolds. In the collagen group, the practical application of bone wax was not feasible because the collagen carrier was not mechanically stable and could not tolerate compression. However, sealing was not necessary because the collagen sponge contained all the liquid within the defect.

Autograft

We harvested autologous bone from the 6 drill holes, which were made with cannulated drill bits at a low rotational speed in order to avoid thermal injury to the autograft and the surrounding bone. The autograft was collected from the grooves of the drill bit. This procedure resulted in a finely-structured graft, which made further processing unnecessary. No periosteum was included, as it was resected from the entire surgical exposure beforehand. The 2 opposing bone defects on either side of the calvaria were filled with 0.701 (SD 0.005) g autograft per 0.785 cm^3 bone defect. Subsequently, we administered 900 IU EPO per defect, or saline.

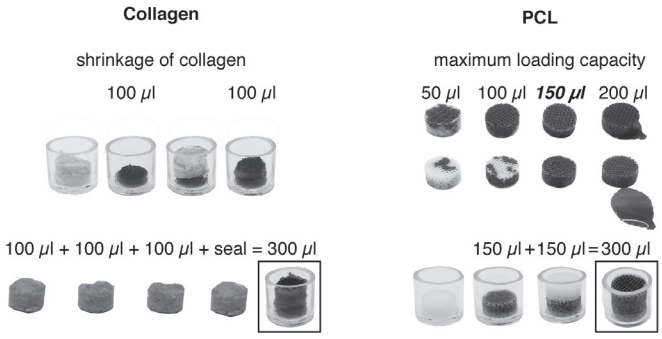

Figure 2. The maximum loading volumes of 100 µL in collagen and 150 µL in PCL scaffolds, and the optimal insertion procedure, were tested in pilot experiments. The sequential insertion and pipetting procedure that was used during the operation is depicted at the bottom of the figure. This procedure assured that there was an even distribution of EPO throughout the collagen carrier and the PCL scaffold.

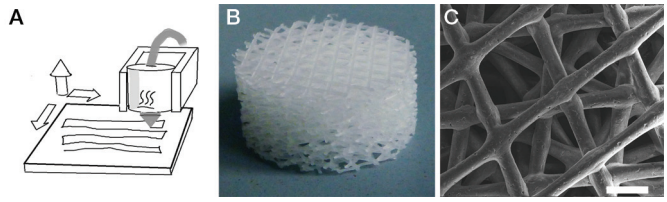

Figure 3. The Bioscaffolder (A) that produced PCL mates from which the PCL scaffolds (10 mm in diameter) were punched (B). Bioscaffolding resulted in a 3-dimensional network of PCL fibers, deposited layer by layer. [Authors: no hyphens here; not an adjective] The individual strands and gaps of the scaffolds were aligned and they were of similar size. This is illustrated by the scanning electron microscopy image (C). Scale bar: 500 µm.

Collagen scaffold

We used a commercially available collagen product, which is resorbed in humans within 3–4 weeks (Sangustop; Aesculap AG, Tuttlingen, Germany). Sangustop is composed of bovine collagen fibrils without any blood serum products or any pharmaceutical activity. 4 cylindrical scaffolds per defect were punched out from the collagen mats with a 10-mm diameter Acu-Punch (Acuderm Inc., Fort Lauderdale, FL) in the operation room. A homogeneously soaked, 4-scaffold-high implant filled the bone defect after 3 rounds of implanting one scaffold at a time and pipetting 100 µL EPO or saline solution on top. The fourth scaffold was inserted as a seal without subsequent pipetting. The reason for this stepwise insertion was the shrinkage of the collagen on exposure to fluid. The optimal insertion strategy and the maximum loading capacity of the collagen and PCL scaffold were determined in pilot experiments (Figure 2).

PCL scaffold

The scaffolds consisted of the polymer polycaprolactone (PCL, MW = 50 kDa; Perstorp, Cheshire, UK). The fiber network of the scaffold was created by rapid prototyping (Bioscaffolder; SysEng, Hünxe, Germany) by extruding the PCL from a needle with an inner diameter of 200 µm (final fiber diameter: ~175 µm) in a layer-by-layer deposition. The deposition speed was 600 mm/min, and distances between fibers were ~1,000 µm (0/105 degree pattern) to allow for a high porosity. The original constructs were made into large rectangular mats from which individual cylindrical scaffolds (diameter: 10 mm; height: 10 mm) were punched out using an Acu-Punch. Next, the scaffolds underwent treatment with 5 M NaOH for 3 h followed by 3 washes with PBS and 2 washes with sterile water for 5 min each on a tilting table. Sterilization took place with 70% ethanol for 16 h. Ethanol was washed out with two 5-min washes with sterile water. The scaffolds were then dried in a sterile desiccator for 3 days. We characterized the constructs using a low-vacuum secondary electron detector (Nova NanoSEM 600; FEI Company, Eindhoven, the Netherlands) and microcomputed tomography (µCT 40; Scanco Medical AG, Zürich, Switzerland) (Chen et al. 2011) (Figure 3). Quality control with these techniques ensured the uniformity of the PCL scaffolds regarding the following parameters: the size of the fibers and pores, the layer-by-layer deposition, the interconnection of the pores, and the homogeneity of the scaffolds.

Anesthesia

Premedication consisted of subcutaneous injection of Zoletil mixture 1 mL/10 kg (tiletamin 2.5 mg/mL, zolazepam 2.5 mg/mL, torbugesic 0.5 mg/mL, ketaminol 2.5 mg/mL, and rompun 2.5 mg/mL). Anesthesia was maintained with 10 mg/kg propofol (10 mg/mL) and 25 µg/kg fentanyl (50 µg/mL).

Surgery

A T-shaped incision measuring 7 × 7 cm was made on the forehead. The periosteum was stripped and resected to reduce spontaneous bone healing via the mesenchymal progenitor cells in the cambium layer (Ozerdem et al. 2003, Holstein et al. 2011). The cranial sutures and lateral borders of the frontal and parietal bone were identified. On each side, 2 bone defects were drilled into the parietal bone and 1 into the frontal bone (Figure 1). The defects were made with a modified 10.0-mm diameter, 3-fluted, cannulated drill bit (cat. no. 360.050; Synthes, Zuchwill, Switzerland). The tip of the drill was flattened and a custom-made adjusting washer stopped advancement beyond 10 mm in depth. These modifications assured a cylindrical bone defect of 10 mm in diameter and 10 mm in depth. Uniform and standardized placement of the defects 1 cm apart, and as far as possible from the sagittal and coronal sutures, was achieved with Kirschner wires, which were placed using wire guides. The position of each bone defect was marked with 2 carbon-fiber rods placed at a distance of 2 mm on the anteromedial and posterolateral side. This safeguard enabled the exact identification of the circumferential and superior borders of the cylindrical defects during tissue processing and analysis. Finally, the 6 defects were treated as described in

Figures 1 and 2. The skin was sutured with a monofilament nylon suture 2-0, disinfected with chlorhexidine, and dressed in a sterile fashion.

Follow-up

Postoperative analgesia was administered subcutaneously 3 times a day for 3 days (buprenorphine, 0.015 mg/kg). Antibiotics were injected daily from 1 day before the operation until the second postoperative day (200,000 IU benzyl penicillin and 200 mg dihydrostreptomycin per 10 kg). Nutrition was restricted to a minimum, but access to water ad libitum was provided. The well-being of the animals and any signs of infection were assessed by professional animal keepers on a daily basis. Blood samples were drawn without anesthesia. An observation time of 5 weeks was chosen based on studies by Jensen et al. (2013) and Stockman et al. (2012). After 5 weeks, a lethal dose of pentobarbital was injected. Subsequently, the frontal and parietal bone was resected en bloc for radiological analysis and further processing.

Outcome measures

The primary outcome measure was bone volume fraction within the defect (BV/TV), determined with high-resolution quantitative computed tomography (HR-QCT) after 5 weeks. Secondary outcome measures were histomorphometric evaluations of the bone defects and blood sample analyses that documented a possible systemic effect of EPO.

Quantitative computed tomography

After en-bloc excision of the parietal and frontal bone, the bone was fixated in chilled 70% ethanol. Subsequent embedding using a modified cold methyl methacrylate (MMA) technique was performed (Erben 1997). The detailed protocol can be found as supplementary material at Acta's website (www.actaorthop.org), identification number 6729.

HR-QCT images of the embedded specimens were acquired with an XtremeCT (Scanco Medical AG, Brüttisellen, Switzerland) with the following parameters: isotropic 82 μm^3 voxel size, 60 kVp, 300 ms integration time, and 900 µA. The images were analyzed with the plugin BoneJ (v.1.3.11) for ImageJ (v.1.47). BoneJ and ImageJ are free, platform-independent, open-source software (Doube et al. 2010, Schneider et al. 2012). No filters were applied. The window level and window width were adjusted automatically. Subsequently, two circular regions of interest (ROIs) were drawn marking the bottom and top of the cylindrical volume of interest (diameter: 10 mm; height: 8.20 mm). The optimal threshold was defined with BoneJ "optimise threshold" for each ISQ file. The mean threshold of these measurements was applied to all ISQ files. Finally, the 2 circular ROIs were interpolated and the BV/TV of the cylinder was determined with BoneJ "volume fraction".

Histomorphometry

According to stereological methodology, the MMA-embedded sections were cut into fixed-axis vertically rotated (FAVER) sections in order to minimize bias (Gundersen et al. 1988, Baas 2008). In brief, the cylindrical, embedded samples were rolled on the table. The surface facing the table was marked, and 5 to 10 consecutive sections were cut parallel to this asymptotic plane. Sections intentionally included the vertical axis, which was the middle of the cylindrical defect. This vertical axis was clearly defined by the groove of the Kirschner wire, which advanced further than the distal boundary of the drill defect. This procedure allowed true 360-degree randomization around the well-defined vertical axis. The 7-µm thick sections were cut on a microtome and subsequently stained with Goldner's Trichrome as previously described (Recker 1983). The rectangular ROI, which encompassed the entire defect, was delineated from the adjacent bone by the clearly identifiable borders of the drill defect.

The following variables were quantified based on the morphological appearance: new bone, old bone, marrow space, osteoid, fibrous tissue, blood vessels, scaffold, and artifacts. Histomorphometry was performed with point counting technique by 2 independent, blinded observers who used an Olympus microscope (Olympus, Ballerup, Denmark) with Visiopharm Integrator System software (newCAST v. 3.4.1.0; Visiopharm A/S, Horsholm, Denmark). The average of 4 counts of the identical ROI by the 2 observers was calculated. Each observer counted 1–3 FAVER sections per defect twice, with more than 7 days between the counts. The intra- and inter-observer variance was determined (Table).

Blood samples

The animals were mildly restrained but not sedated, and central venous blood samples were collected with 4-mL EDTA tubes 1 day before and 1, 2, and 5 weeks after the operation. The animals were not fasting. Blood samples were stored at room temperature until hemoglobin levels, hematocrit, white blood cell count, and platelet count were measured with the fully automatic hematology analyzer Sysmex XE-2100. We did not attempt to measure EPO in the plasma because a previous, unrelated study reported a very low concentration after intravenous administration of 250 IU/kg, which is more than 13 times the concentration in our study (Wu et al. 2012).

Skeletal maturity

There is little scientific evidence concerning skeletal maturity and its implications for preclinical orthopedic animal studies (Rölfing et al., unpublished review). We complied with the newly stipulated recommendations suggesting new standards for reporting skeletal maturity of large animals. In line with the first of these recommendations, the subspecies of swine has been specified above. Secondly, the mean age at the beginning of the observation period has also been specified. Third, the average weight was measured and has been reported above. Fourth, the developmental status of the adjacent growth plates, namely the adjacent cranial sutures, was evaluated with

Results of histomorphometrical analysis: median tissue area fraction (range) and coefficient of variance (CV) in percent

		New bone	Osteoid	Bone marrow	Fibrous tissue	Vessels	Scaffold/Artifacts
Autograft							
Average of observers:	control	55 (44–68)	2.5 (1.1–4.3)	9.6 (4.4–19)	18 (13–28)	0.4 (0.2–1.9)	10 (0.9–21)
	EPO	58 (45–70)	2.7 (0.6–6.1)	9.3 (2.1–23)	21 (7.0–43)	0.6 (0.1–2.7)	9 (2.5–13)
CV [a]	control	4.6; 0.7; 0.7	25; 3.6; 14	24; 0.9; 7.4	18; 0.2; 2.9	44; 26; 15	17; 22; 8.4
	EPO	4.1; 1.7: 1.7	20; 6.4; 2.4	15; 5.0; 5.9	10; 4.3; 1.0	34; 14; 11	20; 21; 5.2
Collagen							
Average of observers:	control	39 (19–57)	3.0 (1.5–9.0)	11 (1.8–20)	43 (20–71)	0.7 (0.2–2.5)	4.2 (2.2–7.0)
	EPO	40 (21–48)	4.5 (2.3–9.3)	6 (0.9–17)	39 (33–73)	1.1 (0.1–1.7)	4.1 (0.9–18)
CV [a]	control	4.6; 2.1; 0.7	13; 2.8; 4.6	18; 6.2; 9.7	8.8; 1.7; 3.9	27; 19; 18	40; 5.6; 14
	EPO	7.3; 1.8; 0.8	18; 1.7; 15	16; 4.8; 6.8	3.0; 3.1; 2.0	56; 33; 36	25; 18; 7.4

[a] Coefficient of variance in percent of inter-observer; intra-observer 1; intra-observer 2

CT scans and histology. Fifth and lastly, we tried to assess the intrinsic healing capacity by including a saline-loaded collagen group in the experiment.

Statistics

HR-QCT and histomorphometic data were analyzed with Wilcoxon paired signed-rank test, because the data were not normally distributed. Before this, histomorphometric data were analyzed with Friedman repeated measures analysis of variance.

Blood sample data were analyzed using one-way repeated measures ANOVA with time as "within-subjects" factor. Normal distribution was confirmed with histograms and QQ-plots. We did not assume sphericity, and therefore used the method of Geisser and Greenhouse. Uncorrected p-values from Fisher's post-hoc tests against the baseline are given. Means are presented with standard deviation (SD) and medians with 95% confidence interval (CI). The coefficients of variance (CV) were calculated as described by Compston et al. (1986). GraphPad Prism v. 6.0b for MacOS X (GraphPad Software, La Jolla, CA) was used for statistical analysis and to prepare graphs.

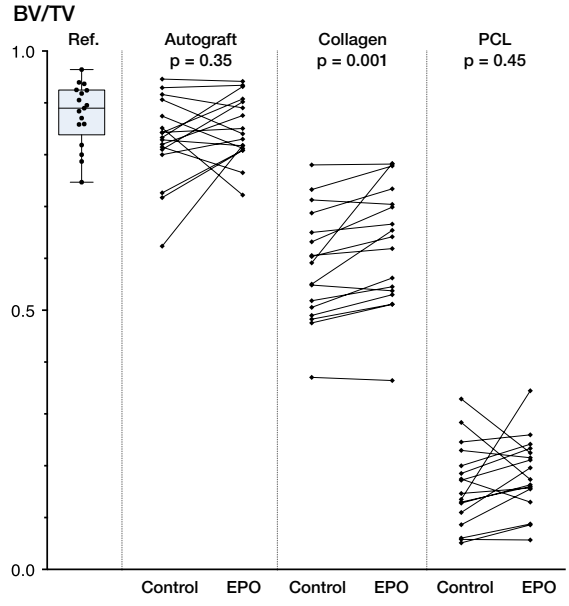

Figure 4. Graphic depiction of BV/TV results assessed with HR-QCT scans (82 µm3 voxel size). Overview of normal calvarial bone, which was used as a reference (ref.) and pairwise comparisons of saline-treated control defects with EPO-treated defects in conjunction with either autograft, a collagen carrier, or a PCL scaffold.

Results (Table)

Observation period

1 animal was killed 5 days postoperatively for reasons unrelated to the cranial surgery. There were no signs of infection at necropsy. An encapsulated, superficial infection was encountered in another animal at the end of the observation period. This infection was accompanied by low weight gain, but without increased white blood cell count or other signs of discomfort. The 6 samples potentially affected were therefore not excluded. Thus, 102 bone defects and 68 blood samples from 17 animals were available for analysis. The average weight at the end of the 35-day observation period was 157 (SD 14) kg.

Quantitative computed tomography

In all animals, the sagittal suture was fused but the cranial suture remained open.

Estimating the EPO/saline ratio, the median BV/TV was 1.01 (CI: 0.97–1.11) in combination with autograft (p = 0.4), 1.06 (CI: 1.02–1.11) when applied on a collagen carrier (p = 0.001), and 1.06 (CI: 0.93–1.45) on the PCL scaffold (p = 0.5) (Figure 4). Notably, a median increase in BV/TV of 6% relative to the control group (BV/TV = 1.0) was observed both in the collagen group and the PCL group. However, statistical significance was only found in the collagen group.

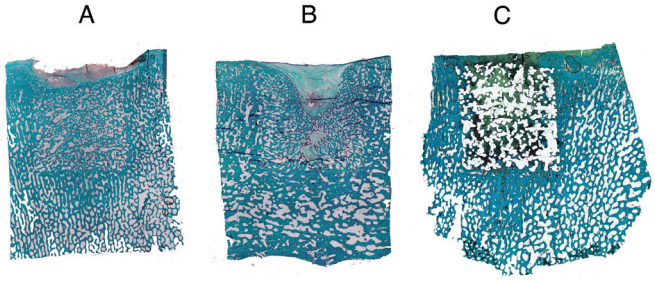

Figure 5. Histological specimens exemplifying the characteristic healing patterns for the 3 groups: autograft (A), collagen carrier (B), and PCL scaffold (C). The intended FAVER section is illustrated in C, where a hyper-dense groove after the centripetal Kirschner wire can be seen. Because no statistically significant differences were found with histomorphometry, random sections with or without EPO are shown.

In absolute values, the excellent healing capability of autograft was apparent, and the BV/TV was not significantly differerent from that of the adjacent calvarial bone, which was used as a reference (Figure 4). The bone healing in the collagen group was substantial and it was statistically significantly augmented after EPO treatment. In contrast, the mineralized ingrowth of bone into the PCL scaffold was sparse, both with and without EPO.

Histomorphometry

The mean point count per ROI was 3,289 (Table).

The majority of PCL specimens disintegrated during the cutting procedure. This was probably due to the scarce tissue ingrowth into the PCL scaffolds. Thus, no representative histological results were obtained. However, we made the qualitative observation that less mineralized bone, and more osteoid and multinucleated cells, were present in PCL sections than in the other groups.

A consistent healing pattern was observed in the collagen group (Figure 5). Bone ingrowth originated mainly from the bottom and the walls of the drill hole. Notably, no old bone was observed in the autograft group, suggesting fast incorporation of the graft.

Consistent with the BV/TV results, the median tissue area fraction of "new bone" was higher in the EPO group than in the control group. However, considering the moderate median effect size of 6%, it was hardly surprising that the methodological variance was larger than the observed biological effect of EPO. Thus, no statistically significant differences between the groups were observed.

No systemic effect of EPO

No statistically significant differences in hematological quantities were observed. The null hypothesis of equal means at all time points was accepted for hematocrit (p = 0.4) and platelet count (p = 0.1), while it was rejected for hemoglobin (p = 0.03) and white blood cells (p = 0.004). Figure 6 shows the individual measurements together with descriptive statistics

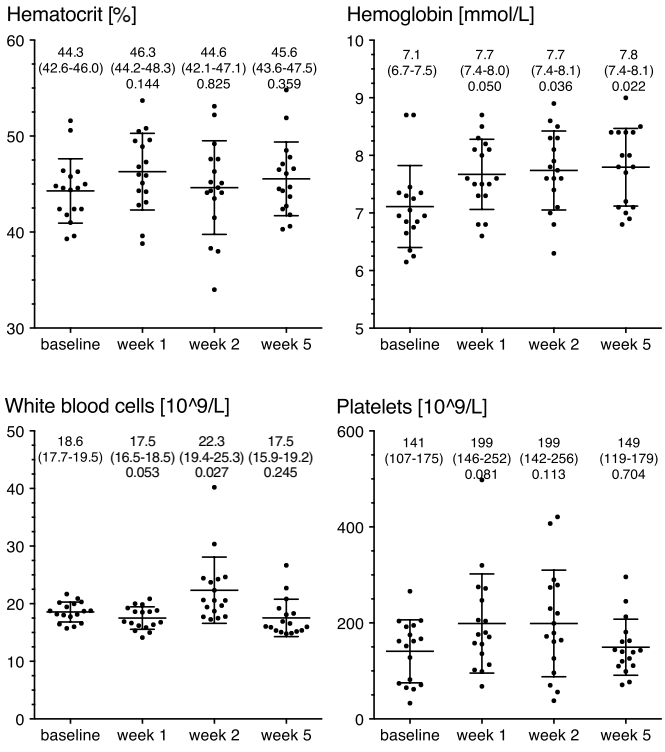

Figure 6. Hematological quantities. The figure shows hemoglobin levels, hematocrit, platelet count, and white blood cell count at baseline and after postoperative weeks 1, 2, and 5. Data are shown as mean ± SD as error bars. Mean, 95% CI, and uncorrected p-value against baseline are given above the graphs. None of the differences were found to be statistically significant following correction for multiple comparisons.

and uncorrected p-values of comparisons of the 3 postoperative time points against baseline.

Briefly, taking multiple comparisons into account, there were no statistically significant differences compared to baseline. However, a minor tendency of increased hemoglobin was observed. The largest observed difference in hemoglobin was 0.68 (CI: 0.11–1.25) mmol/L, which was seen when week 5 was compared with baseline (p = 0.02). The platelet count varied widely, and the automated analyzer frequently suspected clumps. The platelet data should therefore be interpreted with care.

Discussion

To our knowledge, this is the first large-animal study to assess the osteogenic potency of EPO. Furthermore, in contrast to previous studies, we concentrated on possible application of the results to future clinical use, so we used a single topical dose of EPO.

Our main finding was that EPO applied on a collagen carrier increased the median BV/TV fraction by a factor of 1.06 (CI: 1.02–1.11) compared to the saline-treated group. The same

median effect size was found between the PCL groups. However, here the 6% increase in BV/TV did not reach statistical significance. In the bone graft group, 0.7 g autograft per 0.785 cm^3 of bone defect was sufficient to regenerate the bone completely, and independently of the EPO treatment.

The observed effect size was smaller than effect sizes after continuous treatment reported in cell studies and small-animal studies, e.g. 175% and 119% in mineralization of human mesenchymal stromal cells after 21 days of EPO treatment (Kim et al. 2012, Rölfing et al. 2013) and 18% increase in mean bone volume in a rabbit spinal fusion model after 20 injections (Rölfing et al. 2012). This finding is not surprising if the difference between single topical vs. continuous treatment is considered. Another reason for the decreased effect size could be the study design itself. In this paired study, all animals received localized EPO treatment. Despite the absence of statistically significant differences in blood samples, a systemic effect cannot be ruled out. If present, the hypothetical systemic effect may also have positively influenced the control defects and thereby have diminished the differences between EPO groups and control groups. Moreover, it could potentially have masked a transient postoperative drop in hemoglobin levels and hematocrit as observed in previous studies (Rölfing et al. 2012).

In small-animal models, repetitive systemic injections of EPO of up to 6,000 IU/kg/day have been used (Holstein et al. 2007, Shiozawa et al. 2010). However, even significantly smaller cumulative dosing resulted in extremely high blood counts, which invited the concomitant risk of thrombotic events (Ehrenreich et al. 2009, Rölfing et al. 2012). In the present study systemic absorption was limited, as EPO was contained at the defect site—because of the almost avascular nature of the calvaria, and because of the fact that bone defects were sealed with bone wax (Wiltfang et al. 2002). These measures were taken because porcine EPO has 80% DNA sequence homology with human EPO, and several groups have reported hematopoietic and pleiotropic effects of human recombinant EPO in swine (Wen et al. 1993, Kawachi et al. 2012). We studied the effect of EPO compared to within-subject saline controls by performing pairwise comparisons within the collagen carrier group, the autograft group, and the PCL scaffold group, and no comparisons between the 3 different treatment modalities were performed. Thus, sealing with bone wax in the latter 2 groups while the collagen carrier group remained unsealed did not interfere with the results or the interpretation of data.

Concerning the mode of osteogenic action of EPO, we observed a very low percentage of blood vessels (Table). This finding is in agreement with a paper that documented the largely avascular properties of the calvaria (Wiltfang et al. 2002). In addition, and in contrast to our previous small-animal study, the number of blood vessels was not statistically significantly increased (Rölfing et al. 2012). Thus, neovascularization is unlikely to have been a causal factor in the observed increase in BV/TV. We did not assess other means by which EPO promotes bone formation. However, EPO has been shown to directly stimulate osteogenic differentiation of human mesenchymal stromal cells, to exert a chemotactic effect, and to indirectly stimulate bone formation through the secretion of bone morphogenetic proteins from hematopoietic cells (Shiozawa et al. 2010, Rölfing et al. 2013).

The encouraging finding that no significant systemic effect and no adverse effects were observed leads us to the conclusion that the single topical EPO treatment used is safe and moderately effective. Thus, the dose of this study could be used as a guide in planning clinical trials. However, the efficacy of a higher dose, which would possibly be more effective and still clinically safe, should be investigated.

Interestingly, no old bone was observed in the autograft group. The autograft was therefore completely incorporated into the bony structure of the calvaria within 5 weeks of observation. Even so, the delineation between the bone defect and the surrounding bone remained visible on histological sections.

The PCL scaffold was thought to have the possible advantage of combining mechanical strength with a porous structure that would facilitate cellular ingrowth. However, there was very little bony ingrowth into the scaffold and it was not augmented by EPO. In fact, the PCL scaffolds seemed to perform worse than the saline-loaded collagen carrier (Figure 4). The following could partly explain this observation. Firstly, in contrast to the collagen carrier, the PCL scaffold was not degraded, and it therefore took up a large part of the volume inside the defect (Figures 4 and 5). In line with this argument, a previous study in a calvarial defect in swine found that half of the defect volume was occupied by the PCL scaffold after an even longer observation time of 8 weeks (Jensen et al. 2013). Secondly, one can speculate whether the properties of the scaffold inhibited bony ingrowth. For instance, the pore size and the surface topography of PCL are of importance for the ingrowth characteristics of the scaffold (Hulbert et al. 1970, Karageorgiou and Kaplan 2005, Prasad et al. 2013).

Strengths and limitations

Considering that this was a large-animal study with a paired, within-subject design, the group sizes were large ($n_{1-6} = 18$), especially when taking into account that all of these defects were analyzed with all outcome methods at the same time point of 5 weeks. We therefore conclude that the study was not underpowered.

One limitation was that a systemic effect of EPO could not be excluded. Measurement of the concentration of recombinant human EPO in the blood might have been a solution. However, this was not attempted because according to previous reports, 13-fold higher doses of EPO resulted in very low blood levels only (Wu et al. 2012).

Another limitation was that the clearance of EPO from the defect site—and therefore the local concentration—could not be assessed over time. In an earlier in vitro study in which

mesenchymal stromal cells were continuously stimulated with EPO, the highest tested dose of 100 IU/mL EPO had the most pronounced effect. The effect ceased at concentrations below 20 IU/mL. Because of the unknown clearance from the defect, it is difficult to draw conclusions as to how long EPO was present. Further research into the sustained release of 100 IU/mL from scaffold constructs is warranted.

Regarding the external validity, the disparity in osteogenesis between the calvaria and long bones may lead to different results in other bones. However, unlike the human calvaria, the porcine calvaria resembles the human postural skeleton as it shows a trabecular-like structure (Figure 5). Furthermore, endochondral osteogenesis rather than intramembranous bone healing has been observed in a preclinical calvarial model (Sun et al. 2012).

The choice of stereological principles governs the generalizability of the histomorphometric data. Analysis of FAVER sections instead of vertical, uniformly random sections introduces a bias because the peripheral structures within the cylindrical defect are underrepresented compared to centripetal structures (Baas 2008). Furthermore, if the sections do not include the vertical axis, the width of the rectangular ROI decreases. This implies that peripheral structures are likely to be overrepresented compared to true FAVER sections. In the present study, such peripheral structures would be bone ingrowth. Considering that histomorphometry was a secondary outcome evaluation in this study, the feasibility of this methodology outweighed its potential drawbacks.

Conclusion

A single topical dose of EPO increased the median bone volume fraction. The osteogenic effect size of 6% was slightly less than the observed effect after higher, continuous dosing in small-animal models. However, a safe, clinically applicable dose proved to be moderately effective in this porcine calvarial defect model.

Before commencing clinical trials, further large-animal studies that aim to optimize the effect size without compromising the clinical applicability of the treatment regime will be required. Moreover, the ability of EPO to increase bone healing in a more clinically relevant setting, for instance a fracture model of the long bones or a spinal fusion model, remains to be tested in a large-animal model.

Supplementary data

The MMA-embedding protocol is available at Acta's website (www.actaorthop.org), identification number 6729.

JHDR designed the study, performed the surgery, conducted CT and all statistical analyses, and wrote the first draft of the manuscript. JJ performed the surgery, conducted micro-CT analysis, and corrected the manuscript. ASG and JNJ assisted in the surgery, performed histomorphometry, and contributed to the manuscript. HL assisted in the surgery and corrected the manuscript. MC produced and characterized the PCL scaffolds, assisted in the surgery, and proofread the manuscript. LR provided free access to the XtremeCT scanner and proofread the manuscript. CB was the principle investigator involved in planning and finalizing the manuscript.

We thank the following people: Anette Baatrup, Natasja Jørgensen, Jane Pauli, Kirsten Strauss, and the staff at AU Foulum for their technical help; Dang Le for methodological discussions; and Christian Hansen for customization of drills and punches to utmost perfection. We are very grateful to the Department of Clinical Biochemistry and the Department of Forensic Medicine at Aarhus University Hospital, to ConMed Linvatec for supplying us with Hall Powered Instruments, and to B. Braun Medical for providing Sangustop. The study was financed by a grant from the VELUX Foundation.

No competing interests declared.

Baas J. Adjuvant therapies of bone graft around non-cemented experimental orthopaedic implants. Acta Orthop 2008; 79 (suppl 330): 2-43.

Bleuel H, Hoffmann R, Kaufmann B, Neubert P, Ochlich P P, Schaumann W. Kinetics of subcutaneous versus intravenous epoetin-beta in dogs, rats and mice. Pharmacology 1996; 52(5): 329-38.

Bozlar M, Kalaci A, Aslan B, Baktiroglu L, Yanat A N, Tasci A. Effects of erythropoietin on fracture healing in rats. Saudi Med J 2006; 27(8):1267-9.

Chen M, Le D Q S, Baatrup A, Nygaard J V, Hein S, Bjerre L, Kassem M, Zou X, Bünger C. Self-assembled composite matrix in a hierarchical 3-D scaffold for bone tissue engineering. Acta Biomater 2011; 7(5): 2244-55.

Compston JE, Vedi S, Stellon AJ. Inter-observer and intra-observer variation in bone histomorphometry. Calcif Tissue Int 1986; 38(2): 67-70.

Doube M, Kłosowski M M, Arganda-Carreras I, Cordelières F P, Dougherty R P, Jackson J S, Schmid B, Hutchinson J R, Shefelbine S J. BoneJ: Free and extensible bone image analysis in ImageJ. Bone 2010; 47(6):1076–9.

Ehrenreich H, Weissenborn K, Prange H, Schneider D, Weimar C, Wartenberg K, Schellinger P D, Bohn M, Becker H, Wegrzyn M, Jähnig P, Herrmann M, Knauth M, Bähr M, Heide W, Wagner A, Schwab S, Reichmann H, Schwendemann G, Dengler R, Kastrup A, Bartels C. Recombinant human erythropoietin in the treatment of acute ischemic stroke. Stroke 2009; 40(12): e647–56.

Erben R G. Embedding of bone samples in methylmethacrylate: an improved method suitable for bone histomorphometry, histochemistry, and immunohistochemistry. J Histochem Cytochem 1997; 45: 307.

Garcia P, Speidel V, Scheuer C, Laschke M W, Holstein J H, Histing T, Pohlemann T, Menger M D. Low dose erythropoietin stimulates bone healing in mice. J Orthop Res 2011; 29(2): 165-72.

Gundersen H J, Bendtsen T F, Korbo L, Marcussen N, Møller A, Nielsen K, Nyengaard J R, Pakkenberg B, Sørensen F B, Vesterby A. Some new, simple and efficient stereological methods and their use in pathological research and diagnosis. APMIS 1988; 96(5): 379-94.

Holstein J H, Menger M D, Scheuer C, Meier C, Culemann U, Wirbel R J, Garcia P, Pohlemann T. Erythropoietin (EPO): EPO-receptor signaling improves early endochondral ossification and mechanical strength in fracture healing. Life Sci 2007; 80(10):893-900.

Holstein J H, Orth M, Scheuer C, Tami A, Becker S C, Garcia P, Histing T, Mörsdorf P, Klein M, Pohlemann T, Menger MD. Erythropoietin stimulates bone formation, cell proliferation, and angiogenesis in a femoral segmental defect model in mice. Bone 2011; 49(5):1037-45.

Hulbert S F, Young F A, Mathews R S, Klawitter J J, Talbert C D, Stelling F H. Potential of ceramic materials as permanently implantable skeletal prostheses. J Biomed Mater Res 1970; 4(3): 433-56.

Jensen J, Rölfing J H D, Le D Q S, Kristiansen A A, Nygaard J V, Hokland L B, Bendtsen M, Kassem M, Lysdahl H, Bünger C. Surface-modified functionalized PCL scaffolds for bone repair: in vitro and in vivo experiments. J Biomed Mater Res A 2013. Available from: http://doi.org/10.1002/jbm.a.34970.

Karageorgiou V, Kaplan D. Porosity of 3D biomaterial scaffolds and osteogenesis. Biomaterials 2005; 26(27): 5474-91.

Kawachi K, Iso Y, Sato T, Wakabayashi K, Kobayashi Y, Takeyama Y, Suzuki H. Effects of erythropoietin on angiogenesis after myocardial infarction in porcine. Heart Vessels 2012; 27(1): 79-88.

Kim J, Jung Y, Sun H, Joseph J, Mishra A, Shiozawa Y, Wang J, Krebsbach P H, Taichman R S. Erythropoietin mediated bone formation is regulated by mTOR signaling. J Cell Biochem 2012; 113(1): 220-8.

Ozerdem O R, Anlatici R, Bahar T, Kayaselcuk F, Barutcu O, Tuncer I, Sen O. Roles of periosteum, dura, and adjacent bone on healing of cranial osteonecrosis. J Craniofac Surg 2003; 14(3): 371-9.

Prasad A, Berger D, Popat K. PCL nanopillars versus nanofibers: a contrast in progenitor cell morphology, proliferation, and fate determination. Adv Eng Mater 2013; 14: B351–B356.

Recker RR. Bone histomorphometry: techniques and interpretation. CRC Press, Boca Raton, Florida 1983.

Riordan AM, Rangarajan R, Balts JW, Hsu WK, Anderson PA. Reliability of the rabbit postero-lateral spinal fusion model: A meta-analysis. J Orthop Res 2013; 31(8): 1261-9.

Rölfing J H D, Bendtsen M, Jensen J, Stiehler M, Foldager C B, Hellfritzsch M B, Bünger C. Erythropoietin augments bone formation in a rabbit posterolateral spinal fusion model. J Orthop Res 2012; 30(7): 1083-8.

Rölfing J H, Bünger C. Recommendations regarding the rabbit posterolateral spinal fusion model. J Orthop Res 2013; 31(11): 1860.

Rölfing J H D, Baatrup A, Stiehler M, Jensen J, Lysdahl H, Bünger C. The osteogenic effect of erythropoietin on human mesenchymal stromal cells is dose dependent and involves non-hematopoietic receptors and multiple intracellular signaling pathways. Stem Cell Rev 2013. Available from: http://doi.org/10.1007/s12015-013-9476-x.

Schneider C A, Rasband W S, Eliceiri K W. NIH Image to ImageJ: 25 years of image analysis. Nat Methods 2012; 9(7): 671-5.

Schmitt C, Lutz R, Doering H, Lell M, Ratky J, Schlegel K A. Bio-Oss blocks combined with BMP-2 and VEGF for the regeneration of bony defects and vertical augmentation. Clin Oral Implants Res 2013; 24(4): 450-60.

Shiozawa Y, Jung Y, Ziegler AM, Pedersen E A, Wang J, Wang Z, Song J, Wang J, Lee C H, Sud S, Pienta K J, Krebsbach P H, Taichman R S. Erythropoietin couples hematopoiesis with bone formation. PLoS ONE 2010;5(5):e10853.

Stockmann P, Park J, Wilmowsky von C, Nkenke E, Felszeghy E, Dehner J-F, Schmitt C, Tudor C, Schlegel K A. Guided bone regeneration in pig calvarial bone defects using autologous mesenchymal stem/progenitor cells - a comparison of different tissue sources. J Craniomaxillofac Surg 2012; 40(4): 310-20.

Sun H, Jung Y, Shiozawa Y, Taichman RS, Krebsbach P H. Erythropoietin modulates the structure of bone morphogenetic protein 2-engineered cranial bone. Tissue Eng Part A 2012; 18(19-20): 2095-105.

Wen D, Boissel J P, Tracy T E, Gruninger R H, Mulcahy L S, Czelusniak J, Goodman M, Bunn H F. Erythropoietin structure-function relationships: high degree of sequence homology among mammals. Blood 1993; 82(5): 1507-16.

Wiltfang J, Merten H, Schlegel K, Schultze-Mosgau S, Kloss F, Rupprecht S, Kessler P. Degradation characteristics of alpha and beta tri-calcium- phosphate (TCP) in Minipigs. J Biomed Mater Res 2002; 63(2): 115-21.